Inorganic Chemistry

Article

pubs.acs.org/IC

Ferrocenylbenzobisimidazoles for Recognition of Anions and Cations

María Alfonso, Alberto Tárraga,* and Pedro Molina*

Departamento de Química Orgánica, Facultad de Química, Campus de Espinardo, Universidad de Murcia, E-30100 Murcia, Spain

Supporting Information

ABSTRACT: The preparation of 2,7-disubstituted benzobisimidazoles decorated with substituents displaying different electrooptical properties is described. The presence of redox, chromogenic, and fluorescent groups at the heteroaromatic core, which acts as ditopic binding site, made these receptors potential candidates as multichannel probes for ions. The triad **4** behaves as a selective redox and fluorescent chemosensor for HSO_4^- and Hg^{2+} ions, whereas receptor **5** acts as a redox and chromogenic chemosensor molecule for AcO^- and SO_4^{2-} anions. The change in the absorption spectra is accompanied by a color change from yellow to orange, while sensing of Zn^{2+}, Hg^{2+}, and Pb^{2+} cations is carried out only by electrochemical techniques. Receptor **6** exhibits a remarkable cathodic shift of the oxidation wave only in the presence of AcO^-, $H_2PO_4^-$, and $HP_2O_7^{3-}$ anions, whereas addition of Pb^{2+} induces an anodic shift. A new low energy band in the absorption spectra, which is responsible for the color change from colorless to pale yellow, and an important increase of the monomer emission band is observed only in the presence of $H_2PO_4^-$, and $HP_2O_7^{3-}$ anions. The most salient feature of the receptor **6** is its ability to act as a multichannel (redox, chromogenic, and fluorescent) chemodosimeter for Cu^{2+}, and Hg^{2+} metal cations.

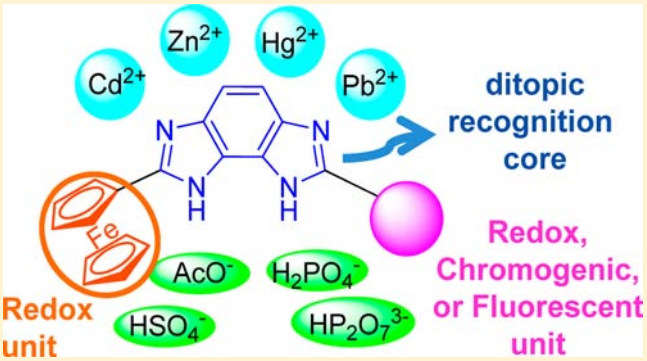

INTRODUCTION

The design of receptors that contain two quite different binding sites for the complexation of cationic and anionic guest species is a new emerging and topical field of supramolecular chemistry.[1] Among different types of chemosensors converting the ion recognition in physical recordable signals, colorimetric/chromogenic chemosensors are especially attractive because the ion recognition can be easily monitored by ion-complexation-induced changes in UV−vis absorption spectra, which would allow the so-called "naked eye" detection of ions. Among organic dyes used as signaling units in the development of chromogenic receptors, dinitrophenyl derivatives have been widely used. However, fluorescence sensors make the best choice, since they are qualified with high sensitivity, fast response, and inexpensive installations, too. As fluorogenic groups, photoactive pyrenyl substituents are very attractive because of long fluorescence lifetime, pure blue fluorescence, strong and well characterized emissions, and their chemical stability.[2] Formation of the self-assembled complex results in a remarkable change in the fluorescence emission intensities of the pyrene excimer and monomer.[3]

Because of its amphoteric nature the imidazole ring behaves as an excellent hydrogen bond donor moiety in synthetic anion receptor systems, and the acidity of the NH proton of the imidazole can be tuned by changing the electronic properties of the imidazole substituents. On the other hand, the presence of a donor pyridine-like nitrogen atom within the ring, capable of selectively binding cationic species also converts the imidazole derivatives into excellent metal ion sensors.[4]

Benzobisimidazoles type **I** with two linear opposed imidazole rings represent a new class of versatile fluorescent compounds,[5] and they have been used as starting material for the preparation of Janus bis(carbenes).[6] Recently, benzobisimidazolium salts have also been shown to act as a redox partner[7] and sensor for CO_2[8] whereas the ferrocene-substituted derivative behaves as a highly selective multichannel chemosensor molecule for acetate anion,[9] and for Pb(II) and Zn (II) metal cations.[10] However, the chemistry of the angular benzobisimidazole isomer II remains almost unexplored,[11] (Chart 1). Only the 2,7-bisferrocene derivative has been proved to be a selective redox and fluorescent chemosensor molecule for hydrogen sulfate and Hg(II) ions.[12]

Ferrocene unit has largely proved to be a simple and remarkable redox-signaling unit. Thus, preparation and sensing properties of ferrocene derivatives have been recently reviewed.[13] In such ferrocene-containing ligands, cation binding at an adjacent receptor site induces a positive shift in the redox potential of the ferrocene/ferrocenium redox couple. The redox-active ferrocene moiety has also been exploited in the electrochemical sensing of anions; these receptors are expected to show cathodic shifts in their redox process when complexed to an anion. Keeping this in mind, decoration of an imidazole derivative with a ferrocene unit could be a valuable way for the electrochemical detections of anions or cations. In this context,

Received: February 12, 2013
Published: June 19, 2013

dx.doi.org/10.1021/ic400365c | Inorg. Chem. 2013, 52, 7487−7496

Chart 1

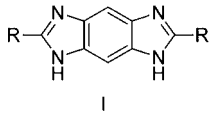

I

2,6-disubstituted-1,7-dihydrobenzo
[1,2-*d*:4,5-*d*′]diimidazole

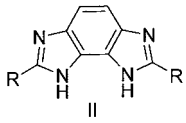

II

2,7-disubstituted1,8-dihydrobenzo
[1,2-*d*:3,4-*d*′]diimidazole

several examples of ferrocenylimidazole derivatives have been successfully used as chemosensor of several kind of ions.[14]

The presence of at least a ferrocenyl group linked to a 2-position of one imidazole ring in benzobisimidazole type II plays a double key role in the recognition event. First, it has been found in several types of aza-substituted ferrocenes that high values of the redox potential shift on coordination are related to the inverse iron−nitrogen separation.[15] Considering the close proximity in structures type **II** between the binding sites of the imidazole ring and the 2-substituted ferrocene unit, important potential shifts of the redox wave of the ferrocene/ferrocenium redox couple should be expected upon either coordination with metal cations or hydrogen-bonded complex formation with anions. Second, it has been recently reported,[16] that electron-rich substituents appended to the 2-position of the imidazole ring increase availability of the N-base electron density, which is an effective means of improving the N-base donor strenght (cation coordination), with concomitant increase of the acidity of the N−H protons of the imidazole ring because of the electron-withdrawing character of the metal ion (anion complexation).

In this context, we report now the preparation, redox and electronic properties as well as anion and cation sensing behavior of a new family of ferrocene receptors, in which the metallocene unit is directly linked to a π-extended imidazole ring such as 1,6-dihydrobenzobisimidazole **II**. At first, this structural motif combines the redox activity of the ferrocene group with the binding ability of the imidazole ring in a highly preorganized system. Our synthetic methodology allows the decoration of the 7-position of this ring system with units displaying different physical properties. The insertion of subunits with different optoelectronic characteristics within the ditopic fluorogenic itself heteroaromatic core may represent an important "added value" to this class of receptors.

The presence of multiple binding sites in the designed new structural motifs, the multiresponsive character of the receptors, and the ability of the imidazole rings to act as a favorable binding site for anions and cations in the recognition event are most noteworthy, allowing their use as multisignaling molecular ion chemosensors.

EXPERIMENTAL SECTION

General Procedure for the Preparation of 2,7-Disubstituted-1,6-dihydrobenzo[1,2-*d*:3,4-*d*′]bisimidazoles 4, 5, and 6. To a solution of 2-ferrocenyl-4,5-diamino-1*H*-benzo[*d*]imidazole (0.20 g, 0.60 mmol) **3**[17] in nitrobenzene (10 mL) the appropriate aldehyde (0.60 mmol) and acetic acid (0.5 mL) were added. The resulting mixture was stirred at 60 °C for 12 h and then a saturated solution of $NaHCO_3$ was added until pH = 7. Then, H_2O (50 mL) was added, and the solution was extracted with CH_2Cl_2 (3 × 50 mL). The organic layer was dried over anhydrous Na_2SO_4 and concentrated to dryness to give a brown residue which was purified on a silica gel column using dicloromethane/hexane/methanol (9:1:0.5) as eluent to afford the corresponding final products, which were crystallized from the adequate solvent.

2,7-Diferrocenyl-1,6-dihydrobenzo[1,2-*d*:3,4-*d*′]bisimidazole 4. Yield: 43% (0.13 g); mp >300 °C (d). ^{1}H NMR (300 MHz, MeOD): δ 4.05 (s, 10H); 4.41 (st, 4H); 5.00 (st, 4H); 7.32 (s, 2H).^{13}C NMR (75 MHz, MeOD) δ: 153.6(C); 135.6 (C); 128.3 (C);

Scheme 1. Synthesis of Receptors 4, 5, and 6[a]

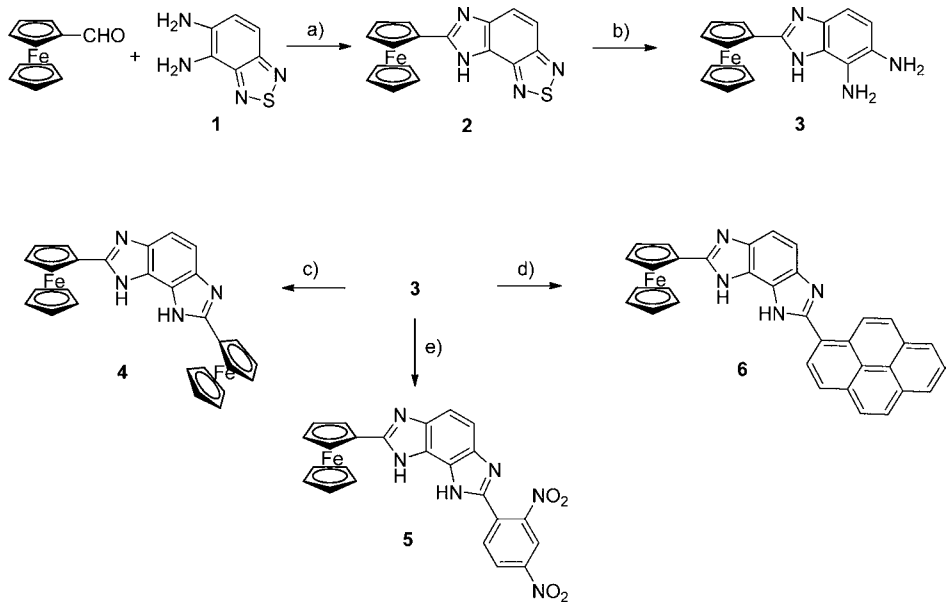

[a]Reagents and conditions: (a) $C_6H_5NO_2$, AcOH, 60 °C; (b) $NaBH_4$, EtOH, $CoCl_2{\cdot}6H_2O$; (c) ferrocenecarboxaldehyde, $C_6H_5NO_2$, AcOH, 60 °C; (d) 2,4-dinitrobenzaldehyde, $C_6H_5NO_2$, AcOH, 60 °C; (e) 1-pyrenecarboxaldehyde, $C_6H_5NO_2$, AcOH, 60 °C.

dx.doi.org/10.1021/ic400365c | *Inorg. Chem.* 2013, 52, 7487−7496

109.9 (CH); 74.3 (C); 71.3 (CH); 70.8 (CH); 68.4 (CH). ESI-MS: 527 (M^++1). Anal. Calc. for $C_{28}H_{22}Fe_2N_4$. C, 63.91; H, 4.21; N, 10.65. Found: C, 63.70; H, 4.45; N, 10.37.

2-Ferrocenyl-7-(2,4-dinitrophenyl)-1,6-dihydrobenzo[1,2-*d*:3,4-*d*′]bisimidazole 5. Yield: 46% (0.14 g); mp = 215−217 °C (d). ^{1}H NMR (400 MHz, CD_3CN) δ: 4.12 (s, 5H); 4.36 (st, 2H); 4.88 (st, 2H); 7.52 (s, 2H), 7.99 (d, J = 8.4 Hz, 1H); 8.37 (dd, J = 1.6, 8.4 Hz, 1H); 8.55 (d, J = 1.6 Hz, 1H). ^{13}C NMR (100 MHz, CD_3CN) δ: 68.0 (CH); 70.4 (CH); 70.7 (CH); 73.0 (C); 74.7(C); 120.6 (CH); 127.3 (CH); 130.6 (C); 132.7 (CH); 144.4 (C); 148.4 (C); 149.4 (C); 153.0 (C). ESI-MS: 509.2 (M^+ + 1). Anal. Calc. for $C_{24}H_{16}FeN_6O_4$. C, 56.71; H, 3.17; N, 16.53. Found: C, 56.50; H, 3.42; N, 16.22.

2-Ferrocenyl-7-(2-pyrenyl)-1,6-dihydrobenzo[1,2-*d*:3,4-*d*′]-bisimidazole 6. Yield: 41% (0.13 g); mp = 240−243 °C (d). ^{1}H NMR (400 MHz, THF-d_8) δ: 4.11 (s, 5H); 4.38 (bs, 2H); 5.09 (bs, 2H); 7.43 (bs, 2H); 8.03 (t, J = 7.8 Hz, 1H); 8.13 (d, J = 9.0 Hz, 1H); 8.16 (d, J = 9.0 Hz, 1H); 8.19 (d, J = 9.6 Hz, 1H); 8.22 (d, J = 9.0 Hz, 1H); 8.24 (d, J = 7.8 Hz, 1H); 8.31 (d, J = 7.8 Hz, 1H); 8.55 (bs, 1H); 9.70 (bs, 1H). Because of solubility problems, the ^{13}C NMR could not be carried out. HR MS (m/z), calculated for $C_{34}H_{22}FeN_4$: 543.1273 (M^++1); found: 543.1276. Anal. Calc. for $C_{34}H_{22}FeN_4$. C, 75.29; H, 4.09; N, 10.33. Found: C, 75.51; H, 3.83; N, 10.50.

RESULTS AND DISCUSSION

Synthesis. Here, we describe the utility of an appropriate diamino-benzothiadiazole **1** as an ideal starting material for building novel angular 2,7-disubstituted benzobisimidazoles decorated with groups displaying different photophysical properties.

Our synthesis started with the preparation of the 4,5-diamino-2,1,3-benzothiadiazole[18] **1** and further condensation with ferrocenecarboxaldehyde to give 7-ferrocenyl-8-*H*-imidazo[4,5-*e*]-2,1,3-benzothiazole[19] **2** in 48% yield. Deprotection of the two amino groups by ring-opening of the thiadiazole ring in compound **2** by reduction with $NaBH_4$ in the presence of $CoCl_2$ provided 2-ferrocenyl-4,5-diamino-1H-benzo[*d*]imidazole[17] **3** in 65% yield. Formation of the second imidazole ring was achieved by reaction with ferrocenecarboxaldehyde, 2,4-dinitrobenzaldehyde, and 1-pyrenecarboxaldehyde to give the 2,7-disubstituted benzobisimidazoles **4** (43%), **5** (46%), and **6** (41%), respectively (Scheme 1).

Sensing Properties. The chemosensor behavior of compounds **4**, **5**, and **6** toward a variety of cations (Li^+, Na^+, K^+, Mg^{2+}, Ca^{2+}, Ni^{2+}, Cu^{2+}, Zn^{2+}, Cd^{2+}, Hg^{2+} and Pb^{2+}), as their perchlorate or triflate salts, (Li^+, K^+, Mg^{2+}, Ni^{2+}, Cd^{2+} and Pb^{2+} were added as perchlorate salts, while Na^+, Ca^{2+}, Cu^{2+}, Zn^{2+}, and Hg^{2+} were added as triflate salts) and anions (F^-, Cl^-, Br^-, AcO^-, NO_3^-, HSO_4^-, $H_2PO_4^-$ and $HP_2O_7^{3-}$ added as TBA$^+$ salts and SO_4^{2-} as tetramethylammonium salt) was investigated by linear sweep voltammetry (LSV), cyclic voltammetry (CV), and Osteryoung square-wave voltammetry[20] (OSWV), as well as through UV−vis, fluorescent and ^{1}H NMR spectroscopic techniques. It is worth mentioning that these recognition studies were carried out in CH_3CN and EtOH solutions for receptors **4** or in CH_3CN solutions in the case of **5**. However, the limited solubility of **6** in those solvents forced us to develop such studies in tetrahydrofuran (THF) solutions.

In recent years alternative mechanisms for several types of anion-receptor interactions[21] have been developed. If the basicity of the anion is insufficient to induce deprotonation of the receptor, one observes formation of a hydrogen-bonded complex manifested in a red-shift of the receptor absorption band and a downfield shift or often disappearance of NMR signals of the receptors protons involved in the hydrogen bonding. If basicity of the anion is high enough to deprotonate the receptor, one observes appearance of a new intense absorption band in the visible region of the electronic spectrum, and the disappearance of NMR signals of abstracted receptor protons, and an upfield shift of the signals of the adjacent protons of the receptor.[22] The titration experiments were further analyzed using the computer program Specfit.[23]

Electrochemical Study. The reversibility and relative oxidation potential of the ferrocene/ferrocenium redox couple in receptors **4**−**6** were determined by cyclic voltammetry (CV), Osteryoung square-wave voltammetry (OSWV), and linear sweep voltammetry (LSV) in solutions of the appropriate solvent containing 0.1 M $[(n\text{-Bu})_4N]PF_6$ as supporting electrolyte.

As expected, the CV of the bis(ferrocene) receptor **4**, shows a reversible two-electron oxidation wave at $E_{1/2}$ = 623 mV, versus the decamethylferrocene (DMFc) redox couple, indicating that the two metal centers are electronically decoupled. Whereas, the electrochemical response of **5** and **6** showed a reversible one-electron oxidation peak at $E_{1/2}$ = 630 mV and $E_{1/2}$ = 675 mV, respectively, versus DMFc (Table 1).

A possible way to reveal the formation of hydrogen-bonded complexes under electrochemical titration conditions is to suppress the deprotonation process by adding a small amount

Table 1. Characteristic Electrochemical Data of the Free Receptors 4−6 and Their Metal and Anion Complexes

compound	$E_{1/2}$ ($\Delta E_{1/2}$)[a]	compound	$E_{1/2}$ ($\Delta E_{1/2}$)[a]
4	623	[**5**·AcO^-]	540 (−90)[b]; 561 (−69)[c]
[**4**·Hg^{2+}]	870 (247)	[**5**·$H_2PO_4^-$]	470 (−160)[b]; 567 (−63)[c]
[**4**·Zn^{2+}]	690 (67)	[**5**·HSO_4^-]	735 (105)[b]; 709 (79)[c]
[**4**·Pb^{2+}]	875 (252)	[**5**·SO_4^{2-}]	490 (−140)[b]; 546 (−84)[c]
[**4**·HBF_4]	895 (275)	[**5**·$HP_2O_7^{3-}$]	404 (−226)[b]; 493 (−137)[c]
[**4**·AcO^-]	487 (−136)[b]; 550 (−73)[c]	[**5**·F^-]	370 (−260)[b]; 579 (−51)[c]
[**4**·$H_2PO_4^-$]	430 (−193)[b]; 529 (−94)[c]	[**5**·OH^-]	355 (−275)
[**4**·HSO_4^-]	667 (44)[b]; 687 (64)[c]	**6**	675
[**4**·SO_4^{2-}]	495 (−128)	[**6**·Zn^{2+}]	747 (72)
[**4**·$HP_2O_7^{3-}$]	365 (−258)[b]; 450(−173)[c]; 480 (−143)[c]	[**6**·Pb^{2+}]	800 (125)
[**4**·F^-]	368 (−255)[b]; 524 (−99)[c]; 573 (−50)[b]	[**6**·Cd^{2+}]	730 (55)
[**4**·OH^-]	269 (−354)	[**6**·AcO^-]	490 (−185)[b]; 552 (−123)[c]
5	630	[**6**·$H_2PO_4^-$]	475 (−200)[b]; 540 (−135)[c]
[**5**·Hg^{2+}]	837 (207)	[**6**·SO_4^{2-}]	508 (−167)[b]; 525 (−150)[c]
[**5**·Zn^{2+}]	720 (90)	[**6**·$HP_2O_7^{3-}$]	450 (−225)[b]; 295 (−380)[b]; 511 (−164)[c]
[**5**·Pb^{2+}]	880 (250)	[**6**·F^-]	523 (−152)[b]; 355 (−320)[b]; 558 (−117)[c]
[**5**·HBF_4]	870 (240)	[**6**·OH^-]	315 (−360)

[a] $\Delta E_{1/2} = E_{1/2\text{complex}} - E_{1/2\text{ free receptor}}$, mV vs DMFc. [b] In the absence of acetic acid. [c] In the presence of 20 equiv of acetic acid.

dx.doi.org/10.1021/ic400365c | Inorg. Chem. 2013, 52, 7487−7496

of acetic acid.[24] In preliminary experiments, we found that addition of up to 20 equiv of acetic acid affected neither CV nor OSWV of receptors **4**, **5**, and **6**.

In all the cases, titration with the strong base Bu_4NOH, which definitely leads to deprotonation, induced a remarkable cathodic shift of the oxidation peak ($\Delta E_{1/2}$ = −354 mV, for **4**, $\Delta E_{1/2}$ = −275 mV, for **5**, and $\Delta E_{1/2}$ = −360 mV, for **6**) (Table 1).

The anion binding properties of **4**, in CH_3CN, demonstrated that only addition of AcO^-, HSO_4^-, and $H_2PO_4^-$ anions promotes remarkable responses. On the other hand, addition of F^-, and $HP_2O_7^{3-}$ anions induced the same change in the oxidation peak as that observed when 1 equiv of Bu_4NOH ($\Delta E_{1/2}$ = −354 mV) was added, which is indicative of the fact that such anions only promote the deprotonation of the free receptor (see Supporting Information, Figures S4–S5). Nevertheless, the results obtained on the stepwise addition of AcO^-, HSO_4^-, and $H_2PO_4^-$ anions revealed three different electrochemical behaviors. For the AcO^- anion a typical "two wave behavior"[25] was observed, with the appearance of a second peak at more negative potential ($\Delta E_{1/2}$ = −136 mV) together with the corresponding to the free receptor. In the case of $H_2PO_4^-$ anion a "shifting behavior" was observed, appearing as a second redox peak, negatively shifted ($\Delta E_{1/2}$ = −193 mV), compared to the free receptor. Remarkably, for HSO_4^- anion a new oxidation peak emerged at more positive potential ($\Delta E_{1/2}$ = +44 mV) (Table 1). The electrochemical behavior observed for HSO_4^- ion is consistent with a guest-to-host proton transfer reaction by the moderately strong acidic HSO_4^- anion, accompanied by hydrogen-bonding and electrostatic interaction with the guest anion: proton transfer is followed by hydrogen-bond formation and subsequent anion coordination.[26]

This assumption is supported by the following results: (a) upon protonation of receptor **4** with HCl the redox peak was shifted anodically ($\Delta E_{1/2}$ = 270 mV); (b) when SO_4^{2-} anion was added, the redox peak was shifted cathodically ($\Delta E_{1/2}$ = −128 mV), and (c) upon addition of SO_4^{2-} anion to the electrochemical solution of the protonated receptor [**4**·H^+] a cathodically shifted oxidation peak appears at virtually the same potential as that observed for the [**4**·HSO_4^-] complex ($E_{1/2}$ = 667 mV) (Figure 1)

On the other hand, the results obtained on the stepwise addition of substoichiometric amounts of the above-mentioned set of metal cations show that only the addition of Hg^{2+} and Zn^{2+} induced the appearance, in the OSWV, of a new oxidation peak at a remarkably more positive potential (Table 1). In the case of Pb^{2+} a new oxidation peak was also observed in the OSWV at $E_{1/2}$ = 875 mV. However, the reduction peak in the CV of the complex **4**·Pb^{2+} appears at a potential which is almost the same as that observed for the free receptor. This experimental result could be explained in the following way: once the oxidation of the ferrocene unit present in the formed complex **4**·Pb^{2+} has taken place, such species is almost completely disrupted and therefore the Pb^{2+} ion is expelled from the receptor. As a consequence, the reduction will take place on the radical cation $\mathbf{4}^+$ derived from the free receptor **4**. In other words, this result shows that the **4**·Pb^{2+} complex undergoes reversible electrochemically induced complexation/decomplexation processes on a time scale faster than the electrochemical experiment (see Supporting Information, Figure S8).

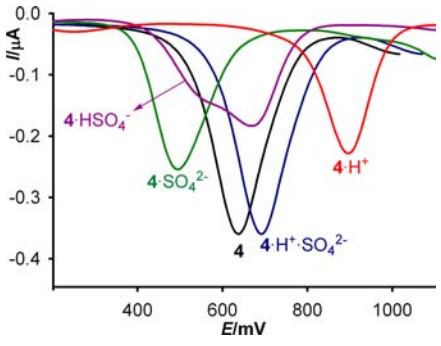

Figure 1. Evolution of the OSWV of **4** ($c = 1 \times 10^{-4}$ M) in CH_3CN/*n*-Bu_4NPF_6, versus decamethylferrocene (DMFc) redox couple, scanned at 0.1 V s^{-1} in the presence of (a) HSO_4^- (purple); (b) HCl (red); (c) SO_4^{2-} (green); (d) initial addition of HCl followed by addition of SO_4^{2-} (blue).

Interestingly, while addition Zn^{2+}, Pb^{2+}, and Hg^{2+} metal cations to **4** promotes the formation of the corresponding complexes, addition of Cu^{2+} induces the oxidation of the ferrocene moiety present in the free receptor.

With reference to the electrochemical titration studies carried out by using receptor **5**, it is worth highlighting that addition of AcO^-, $H_2PO_4^-$, HSO_4^-, and SO_4^{2-} anion, in the presence of acetic acid, induced the same kind of perturbation in the oxidation potential as those observed with receptor **4**. These electrochemical data also suggest that the interaction of the HSO_4^- anion with receptor **5** also involves an initial proton transfer followed by hydrogen-bond formation and subsequent anion coordination. Addition of F^- and $HP_2O_7^{3-}$ anions definitely lead to deprotonation and induced a strong cathodic shift of the oxidation peak.

Likewise, addition of the above-mentioned metal cations to an electrochemical solution of receptor **5** in CH_3CN show that only the addition of Hg^{2+}, Pb^{2+}, and Zn^{2+} induced the appearance, in the OSWV, of a new oxidation peak at a remarkably more positive potential (Table 1). Again, the potential of the reduction peak in the CV of [**5**·Pb^{2+}] also resembles that of the free receptor, and addition of Cu^{2+} metal cation promotes the same oxidation effect observed when the receptor **4** was used.

The electrochemical recognition abilities of **6** were also investigated in the presence of anions and cations. The results obtained demonstrate that the oxidation wave associated to the free receptor underwent a cathodic shift upon addition of AcO^-, H_2PO_4, and SO_4^{2-} anions although the magnitude of those shifts and the electrochemical behavior were dependent on the anion studied. Thus, addition of substoichiometric amounts of SO_4^{2-} anion revealed a typical "two wave behavior", with the appearance of a second peak at more negative potential together with the one corresponding to the free receptor (see Supporting Information, Figure S17). By contrast, the addition of the other oxoanions gave rise to a "shifting behavior", in which a second redox peak, cathodically shifted when compared to the free receptor, appears (Figure 2 and Table 1).

Addition of $HP_2O_7^{3-}$ and F^- to **6** induced the progressive appearance of two new oxidation peaks cathodically shifted. To rule out possible deprotonation processes of the free ligand, we have also carried out other electrochemical experiments either by adding Bu_4NOH to the electrochemical solution of the free receptor or by titrating with these anions in the presence of acetic acid, in which case the deprotonation process is

dx.doi.org/10.1021/ic400365c | Inorg. Chem. 2013, 52, 7487–7496

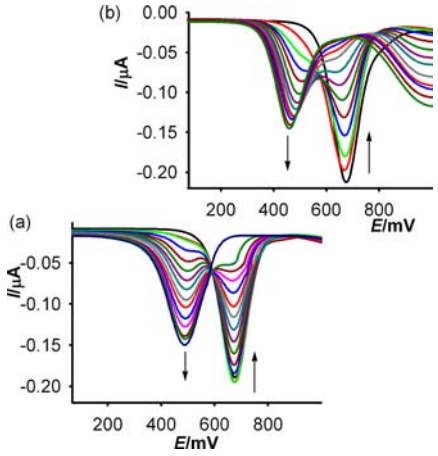

Figure 2. Evolution of the OSWV of **6** ($c = 2 \times 10^{-4}$ M in THF), using n-Bu_4NPF_6 as supporting electrolyte and scanned at 0.1 V s^{-1}, upon addition of increasing amounts of (a) $[(n\text{-Bu})_4N]AcO$ and (b) $[(n\text{-Bu})_4N]H_2PO_4$.

prevented. First, titration with the strong base Bu_4NOH gave rise to the appearance of a new oxidation peak, cathodically shifted. This magnitude is quite similar to that obtained for the cathodic shift of one of the oxidation peaks resulting upon addition of $HP_2O_7^{3-}$ and F^-, but different as those derived from the addition of AcO^-, $H_2PO_4^-$, and SO_4^{2-} anions. Second, titrations in the presence of 20 equiv of AcOH almost did not affect the results obtained in the electrochemical titrations carried out by using AcO^-, $H_2PO_4^-$, and SO_4^{2-} anions alone, whereas addition of $HP_2O_7^{3-}$ or F^- to an electrochemical solution of receptor **6**, under the same acidic conditions, gave only rise to one oxidation peak, cathodically shifted (see Supporting Information, Figure S18). These data clearly suggest that the perturbations observed upon addition of AcO^-, $H_2PO_4^-$, and SO_4^{2-} anions to the free receptor **6** should be associated to a recognition event, involving the formation of a hydrogen-bonded complex between **6** and such anions. On the other hand, the results obtained upon titration with $HP_2O_7^{3-}$ and F^- anions showed that in the absence of an acidic medium both a deprotonation and a recognition process should simultaneously taking place, while in the presence of a small amount of acetic acid only the corresponding hydrogen-bonded complexes are formed (Table 1).

The results obtained from the electrochemical metal cation binding studies of **6** show that only the progressive addition of Zn^{2+}, Cd^{2+}, and Pb^{2+} metal cations promote a significant anodic shift of the ferrocene oxidation peak in the free receptor. Once again, the $[\mathbf{6}\cdot Pb^{2+}]$ complex formed is almost completely disrupted when such complex undergoes electrochemical oxidation and, consequently, the Pb^{2+} is then expelled from the receptor. Moreover, the substantial shift toward cathodic currents observed in the corresponding LSV of the free receptor upon addition of Cu^{2+} and Hg^{2+} constitutes a relevant evidence of the oxidant character of these metal cations toward **6** (see Supporting Information, Figures S19–S20).

Absorption and Emission Study. Ion recognition properties of the receptor **4** toward metal cations and anions have also been studied by using absorption and emission techniques. The

Table 2. Characteristic UV-vis Data for the Receptor 4–6 and Representative Metal and Anion Complexes

receptor	UV–vis λ_{max} (10^{-3} ε)[a]	IP[b]	K_{as}	D_{lim}[c]
4[d]	304 (1.721); 445 (0.068)			
$[\mathbf{4}\cdot Zn^{2+}]$[e]	304 (1.776); 460 (0.098)	319		
$[\mathbf{4}\cdot Cd^{2+}]$[e]	304 (1.830); 455 (0.100)	319		
$[\mathbf{4}\cdot Cu^{2+}]$[e]	366 (0.574); 430 (0.469); 915 (0.117)	290; 335		
$[\mathbf{4}\cdot Hg^{2+}]$[f]	304 (1.504); 455 (0.094)		9.46×10^{4}[i]	5.26×10^{-6}
$[\mathbf{4}\cdot HBF_4]$[f]	304 (1.705); 445 (0.112)	319; 337		
$[\mathbf{4}\cdot H_2PO_4^-]$[d]	304 (1.588); 448 (0.061)			
$[\mathbf{4}\cdot SO_4^{2-}]$[d]	304 (1.394); 448 (0.066)			
5[e]	307 (1.099); 390 (0.694)			
$[\mathbf{5}\cdot Pb^{2+}]$[e]	310 (1.317); 358 (sh)	372	1.28×10^{5}[i]	1.02×10^{-5}
$[\mathbf{5}\cdot HBF_4]$[e]	358 (sh); 455 (0.088)	355		
$[\mathbf{5}\cdot Cu^{2+}]$[e]	374 (0.854); 923 (0.061)	320		
$[\mathbf{5}\cdot AcO^-]$[e]	307 (1.099); 419 (0.681)	403	4.80×10^{4}[i]	7.48×10^{-6}
$[\mathbf{5}\cdot H_2PO_4^-]$[e]	307 (1.096); 413 (0.675)	403	4.99×10^{5}[i]	5.03×10^{-6}
$[\mathbf{5}\cdot SO_4^{2-}]$[e]	307 (1.064); 428 (0.676)	403	9.97×10^{4}[i]	6.53×10^{-6}
$[\mathbf{5}\cdot HP_2O_7^{3-}]$[e]	310 (1.047); 485 (0.925)	418		
$[\mathbf{5}\cdot OH^-]$[e]	310 (1.058); 485 (0.887)	313; 342; 418		
6[g]	300 (1.685); 374 (1.589)			
$[\mathbf{6}\cdot Zn^{2+}]$[g]	351 (1.468); 455 (0.057)	315; 360; 440	1.09×10^{12}[j]	1.05×10^{-5}
$[\mathbf{6}\cdot Pb^{2+}]$[g]	365 (1.719); 455 (0.067)	300; 315; 375; 435	3.28×10^{6}[i]	6.41×10^{-6}
$[\mathbf{6}\cdot Hg^{2+}]$[g]	362 (1.742); 455 (0.072); 940 (0.070)			
$[\mathbf{6}\cdot Cu^{2+}]$[g]	360 (1.462); 940 (0.075)	290		
$[\mathbf{6}\cdot AcO^-]$[g]	310 (1.435); 385 (1.442); 400 (sh, 1.341)	330; 385		
$[\mathbf{6}\cdot H_2PO_4^-]$[g]	310 (1.436); 385 (1.420); 400 (sh, 1.267)	330; 385		
$[\mathbf{6}\cdot HP_2O_7^{3-}]$[g]	307 (1.426); 385 (1.443); 400 (sh, 1.301)[h]	310; 330; 385	3.57×10^{4}[i]	4.36×10^{-6}
$[\mathbf{6}\cdot F^-]$[g]	303 (1.449); 385 (1.468); 400 (1.253)[h]	310; 330; 385	2.28×10^{5}[i]	9.61×10^{-6}
$[\mathbf{6}\cdot OH^-]$[g]	385 (1.362); 405 (sh, 1.235)	330; 385		

[a] ε in dm^3 mol^{-1} cm^{-1}. [b] Isosbestic points in nm. [c] Detection limits in M. [d] CH_3CN or EtOH solution. [e] CH_3CN solution. [f] EtOH solution. [g] THF solution. [h] In the presence of 20 equiv of acetic acid. [i] In M^{-1}. [j] In M^{-2}.

dx.doi.org/10.1021/ic400365c | Inorg. Chem. 2013, 52, 7487–7496

UV−vis absorption spectrum of receptor **4** in CH_3CN ($c = 5 \times 10^{-5}$ M) and EtOH at the same concentration, exhibits two bands at $\lambda = 304$ nm ($\varepsilon = 1721$ M^{-1} cm^{-1}) and 445 nm ($\varepsilon = 68$ M^{-1} cm^{-1}) (Table 2 and Supporting Information, Table S1). The addition of Mg^{2+}, Ni^{2+}, Zn^{2+}, Cd^{2+}, Hg^{2+}, and Pb^{2+} elicited the same optical response: the progressive appearance of a new LE band red-shifted by $\Delta\lambda = 5-15$ nm and well-defined isosbestic points indicative of the presence of only two absorbing species in the solution were found (Supporting Information, Figure S21). However, in EtOH solution only the addition of Hg^{2+} cations induced the red-shift of the LE band by $\Delta\lambda = 10$ nm (Supporting Information, Figure S24). Binding assays using the method of continuous variations (Jobs plot) suggest a 1:1 binding model (Supporting Information, Figure S25). Titration studies of receptor **4** toward the set of anions under study revealed that only F^-, AcO^-, SO_4^{2-}, $H_2PO_4^-$, and $HP_2O_7^{3-}$ decrease in the intensity of the HE absorption band (see Supporting Information, Figure S26).

Assessments of the ion affinities also came from observing the extent to which the fluorescence intensity of the receptor **4** was affected in the presence of cations and anions (see Supporting Information, Figure S28). As expected, receptor **4** showed a weak fluorescence in EtOH ($c = 10^{-5}$ M), revealing that the excitation spectrum at $\lambda = 330$ nm is an ideal excitation wavelength. The emission spectrum displays a structureless band centered at $\lambda = 405$ nm, with a rather low quantum yield ($\Phi = 10^{-3}$) with reference to anthracene as standard ($\Phi = 0.27 \pm 0.001$).[27] Receptor **4** in EtOH showed a large CHEF (**C**helation-**E**nhanced **F**luorescence **E**ffect)[28] when Hg^{2+} cation was added. Thus addition of 1 equiv of Hg^{2+} cation induced a red-shift ($\Delta\lambda = 10$ nm) of the emission band which is also accompanied by a remarkable increase in the intensity of such emission band (CHEF = 225), and by a 60 fold increase in the quantum yield ($\Phi = 6 \times 10^{-2}$) (see Supporting Information, Figure S29). From the fluorescence titration data, a 1:1 binding mode is deduced, and the association constant was calculated to be 3.95×10^5 M^{-1}. The detection limit[29] was found to be 6.58×10^{-6} M.

After addition of 1 equiv of HSO_4^- anion to a solution of the receptor **4** in EtOH, the emission band red-shifted ($\Delta\lambda = 13$ nm), with a concomitant increase in the intensity of the emission band (CHEF = 486), and in the fluorescence quantum yield which increased by a factor of 100 ($\Phi = 10^{-1}$) (Figure 3). The stoichiometry of the complex was also determined by the changes in the fluorogenic response of **4** and

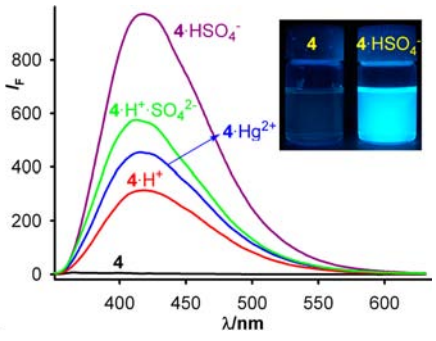

Figure 3. Evolution of the emission spectrum of **4** (black), upon addition of (a) HSO_4^- (purple); (b) HBF_4 (red); (c) initial addition of HBF_4 followed by addition of SO_4^{2-} (green); (d) Hg^{2+} (blue). Inset: visual features observed upon addition of HSO_4^- anion.

HSO_4^- anion, the results indicating the formation of 1:1 complex with association constant $K_a = 4.19 \times 10^4$ M^{-1} and detection limit 1.57×10^{-6} M.

Interestingly, the protonated species [**4**·H^+], formed by addition of 1 equiv of HBF_4 to the free ligand, showed the same emission spectrum as those obtained by addition of both Hg^{2+} and HSO_4^- ions, although with a CHEF = 156 (Figure 3). Moreover, the emission band of [**4**·H^+] undergoes a gradual increase in intensity only upon addition of SO_4^{2-} ion, reaching a maximum when 1 equiv of this anion was added (CHEF = 1.83). This result clearly indicates that the protonated species [**4**·H^+] could be used for the selective detection of SO_4^{2-} ion, taking into account that the only addition of this anion to the free ligand does not promote any change in its emission spectrum (Figure 3).

The stoichiometries proposed from absorption and fluorescent data were further confirmed by mass spectrometry. The ESI mass spectrum of receptor **4** in the presence of HSO_4^- shows a peak at m/z 623.5 corresponding to the 1:1 complex, whereas the ESI and ESITOF mass spectra in the presence of Hg^{2+} cations show a peak at m/z 1451 corresponding to the complex [**4**·Hg^{2+}]$_2$. The relative abundance of the isotopic clusters was in good agreement with the simulated spectra of the complexes (see Supporting Information, Figures S32−S35).

The UV−vis absorption spectrum of receptor **5** in CH_3CN ($c = 5 \times 10^{-5}$ M) exhibits two bands at $\lambda = 307$ nm ($\varepsilon = 1099$ M^{-1} cm^{-1}) and 390 nm ($\varepsilon = 694$ M^{-1} cm^{-1}). The addition of Zn^{2+}, Hg^{2+}, and Pb^{2+} elicited the same optical response: the progressive appearance of a new LE band blue-shifted ($\Delta\lambda = -32$ nm), and the initial yellow solution of the receptor becomes colorless (Figure 4). The presence of well-defined

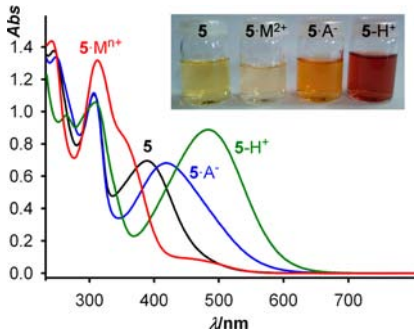

Figure 4. Changes in the absorption spectra of **5** (black) ($c = 5 \times 10^{-5}$ M in CH_3CN) upon addition of increasing amounts of: $Pb(ClO_4)_2$; $Zn(OTf)_2$ and $Hg(OTf)_2$ (deep red); [(*n*-Bu)$_4$N]AcO, [(*n*-Bu)$_4$N]$_2$$SO_4$ and [(*n*-Bu)$_4$N]H_2PO_4 (deep blue); [(*n*-Bu)$_4$N]F, [(*n*-Bu)$_4$N]$_3$$HP_2O_7$ and [(*n*-Bu)$_4$N]OH (deep green). Inset: visual features observed upon addition of metal cations, anions, and upon deprotonation.

isosbestic points indicates the existence of only two absorbing species in the solution. Binding assays using the method of continuous variations (Job's plot) suggest a 1:1 binding model for Pb^{2+} (Supporting Information, Figure S37). Electrospray mass spectra also confirmed such stoichiometries because they show the appropriate molecular ion peaks with the relative abundance of the isotopic clusters being in good agreement with the simulated spectra of the complexes formed (see Supporting Information, Figures S38−S41).

Titration studies of receptor **5** toward the set of anions under study revealed that only AcO^-, $H_2PO_4^-$, and SO_4^{2-} ions

dx.doi.org/10.1021/ic400365c | Inorg. Chem. 2013, 52, 7487−7496

induced the progressive appearance of a new LE band red-shifted ($\Delta\lambda$ = 29 nm for AcO^-, $\Delta\lambda$ = 23 nm for $H_2PO_4^-$, and $\Delta\lambda$ = 38 nm for SO_4^{2-} ion) (Figure 4). A well-defined isosbestic point at λ = 403 nm indicated that a neat interconversion between the uncomplexed and complexed species occurs. The new LE band is responsible for the change of color, from yellow to orange, which can be used for "naked eye" detection of these anions. From analysis of the spectral titrations data and electrospray mass spectra studies (see Supporting Information, Figures S43–S47), 1:1 binding stoichiometries were determined and the binding constants were determined (Table 2). The absorption spectrum of **5** in the presence of either F^- or $HP_2O_7^{3-}$ displayed the same changes as those observed with Bu_4NOH: the appearance of a new red-shifted band ($\Delta\lambda$ = 95 nm), which is responsible for the strong red color of the deprotonated species **5**-H^+ (Figure 4).

The recognition capacity of **6** toward anions and cations was also studied by observing changes in their UV–vis absorption and emission spectra. When a THF solution of **6** ($c = 5 \times 10^{-5}$ M) was titrated with AcO^-, $H_2PO_4^-$, $HP_2O_7^{3-}$, and F^- anions, the absorption band centered at 374 nm gradually decreased and two new lower energy absorption bands emerged at 385 nm (ε = 1440 M^{-1} cm^{-1}) and 400 nm (ε = 1315 M^{-1} cm^{-1}), with clear isosbestic points. The new LE absorption band appearing at 400 nm is responsible for the color change of the solution from colorless to pale yellow. As an example, Figure 5

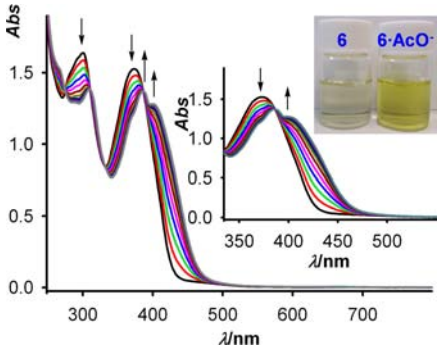

Figure 5. Changes in the absorption spectra of **6** ($c = 5 \times 10^{-5}$ M in THF) upon addition of increasing amounts of [(*n*-Bu)$_4$N]AcO until 1.8 equiv were added. Inset: visual features observed after addition of AcO^- anions.

displays the spectra obtained on titration with $[Bu_4N]AcO$, although these spectral features are the same as those observed for the other mentioned anions (see Supporting Information, Figure S50).

The Job's plots display a maximum absorption change when the molar fraction of A versus [**6** + A] (A = AcO^-, and $H_2PO_4^-$) is 0.5, indicative of the formation of the corresponding complexes with 1:1 stoichiometry (see Supporting Information, Figure S51). The association constants were calculated (Table 2) from these titration data. Taking into account that upon addition of F^- and $HP_2O_7^{3-}$ only hydrogen-bonded complex formation takes place in the presence of acetic acid, the Job's plots were obtained under such conditions and demonstrated that binding between receptor **6** and these anions also occurs through a 1:1 stoichiometry. From these titration data, the apparent association constants were calculated. In the case of AcO^- and $H_2PO_4^-$ such stoichiometry has also been further confirmed by analysis of the electrospray mass spectra of the complexes [**6**·A] (A = AcO^-, and $H_2PO_4^-$) which show molecular ion peaks at m/z 601.5 and 639.0, respectively. Moreover, the relative abundance of the isotopic clusters was in good agreement with the simulated spectra of the complexes (see Supporting Information, Figures S52–S54).

When titrations were carried out in the presence of AcOH, only F^-, AcO^-, and $HP_2O_7^{3-}$ anions promoted the same slight bathochromic shift of the LE band observed under neutral conditions (see Supporting Information, Figure S55).

When the titration experiments were carried out with metal cations, the receptor **6** only responded to the presence of Zn^{2+}, Cd^{2+}, and Pb^{2+}. In these cases, a new and weak absorption band centered at 455 nm developed on titration, and sharp isosbestic points were observed (see Supporting Information, Figure S56). The titration profiles could be fitted to a 1:1 (ligand:metal cation) model for Cd^{2+} and Pb^{2+} and to a 2:1 stoichiometry for Zn^{2+} (Supporting Information, Figure S57).

The oxidation experienced by receptors **4** and **5** in the presence of Cu^{2+} and **6** upon addition of Cu^{2+} and Hg^{2+} has also been confirmed by UV–vis experiments. The resulting spectra obtained from the oxidation of **4** and **5** with Cu^{2+} and from **6**, both with Cu^{2+} and Hg^{2+}, gave rise to a new band in the region 915–940 nm, which can be ascribed to the formation of a ferrocenium ion[30] (see Supporting Information, Figure S58).

The changes in the fluorescence spectrum of **6** upon addition of metal cations and anions were also examined. Receptor **6** ($c = 5 \times 10^{-6}$ M in THF) shows a weak and structureless monomer emission band at 449 nm (Φ = 0.015) when excited at 380 nm. On addition of increasing amounts of anion, receptor **6** only shows reliable changes upon addition of $H_2PO_4^-$ and $HP_2O_7^{3-}$ anions, consisting in the appearance of a new and more intense red-shifted emission band ($\Delta\lambda$ = 22 nm, Φ = 0.111 for $H_2PO_4^-$, and $\Delta\lambda$ = 36 nm, Φ = 0.206, for $HP_2O_7^{3-}$) (Figure 6). Similar results were also obtained when

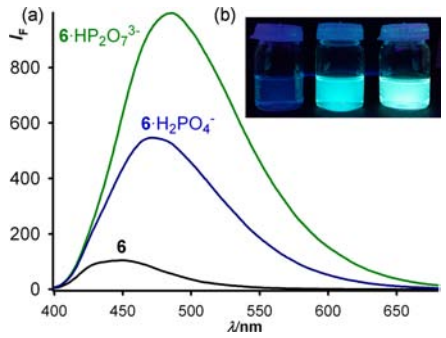

Figure 6. (a) Changes in the emission spectra of **6** ($c = 5 \times 10^{-6}$ M in THF) in the presence of 2 equiv of the indicated species. Emission is monitored at λ_{exc} = 380 nm. (b) Visual changes observed in the fluorescence of THF solutions of **6** (left) after addition of [(*n*-Bu)$_4$N]H$_2$PO$_4$ (middle) and [(*n*-Bu)$_4$N]$_3$HP$_2$O$_7$ (right).

such titration processes were carried out in the presence of AcOH, confirming the recognition event taken place between receptor **6** and those anionic species (see Supporting Information, Figures S59–S61 and Table S2). The 1:1 stoichiometry of the complexes was also confirmed by fluorescence Job's plots, the calculated association constants being $K_{as} = 4.26 \times 10^5$ M^{-1} for the case of $H_2PO_4^-$ and $K_{as} = 2.60 \times 10^6$ M^{-1} for $HP_2O_7^{3-}$ anions.

The fluorogenic metal ion binding properties of **6** demonstrate that the fluorescence emission was only affected

dx.doi.org/10.1021/ic400365c | Inorg. Chem. 2013, 52, 7487–7496

by the presence of Cu^{2+} and Hg^{2+} metal cations as a consequence of the oxidation of the ferrocene. In these cases, the change in emission of **6** also results in both an increase of the fluorescence intensity (CHEF = 6 for Cu^{2+} and CHEF = 5 for Hg^{2+}) and a deep change in intensity of the blue color of the receptor solution (Figure 7). Such interesting results may be

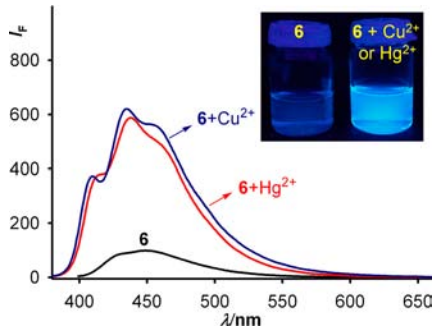

Figure 7. Changes in the emission spectra of **6** ($c = 5 \times 10^{-6}$ M in THF) in the presence of Cu^{2+} or Hg^{2+} cations. Inset: visual changes observed upon oxidation of **6** by these metal cations.

explained by quenching of the fluorescence of the pyrene subunit in the neutral triad **6** by the ferrocene moiety[31] which is responsible for the weak emission band observed. However, after oxidation of **6**, the electron-donating ability of the ferrocene moiety is reduced and, as a result, the electron transfer is arrested leading to a fluorescence enhancement. So that, receptor **6** behaves as a multichannel chemodosimeter of these metal cations. Also, as the ferrocene/ferrocinium pair transformation in **6** can be reversibly carried out, the possibility of obtaining a redox-fluorescent switch, based on the triad **6**, is opened.

^{1}H NMR Study. To gain some insight about the plausible binding modes operating in these recognition processes, a ^{1}H NMR titration study of **4** in CH_3OD solutions was also carried out (Figure 8). The results obtained in this study demonstrated

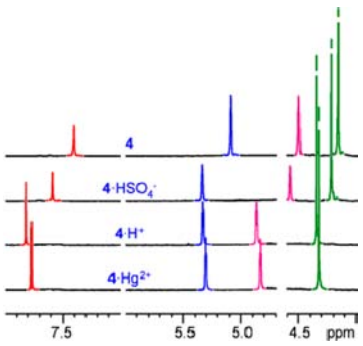

Figure 8. Evolution of the ^{1}H NMR spectrum of **4** upon addition of 1 equiv of HSO_4^-, HBF_4, and $Hg(OTf)_2$.

a similar trend upon addition of both Hg^{2+} and HSO_4^- ions to the free ligand. Thus, the progressive addition of Hg^{2+} to the solution of **4** in CH_3OD causes the simultaneous downfield shift of the ferrocene protons and those signals associated to the central ring protons. The maximum downfield shifts were observed when addition of 1 equiv of Hg^{2+} was reached: $\Delta\delta H_{Cp}$ = 0.19 ppm, $\Delta\delta H_{\alpha}$ = 0.21 ppm, $\Delta\delta H_{\beta}$ = 0.36 ppm, and $\Delta\delta H_{Ph}$ = 0.36 ppm. More importantly, similar changes in the chemical shifts of these protons were also observed when HSO_4^- anion was added, which indicate that this anion interacts with the free ligand promoting a protonation process on the imidazole nitrogen atoms.

Moreover, the ^{1}H NMR spectra of **4** upon addition of increasing amounts of HBF_4 also displayed the same set of signals as those observed for the species formed upon addition of both Hg^{2+} and HSO_4^- ions (see Supporting Information, Figures S64–S66 and Table S3). Consequently, we assume that addition of HSO_4^- ions promotes, in a first stage, the *N*-protonation of the imidazole moiety which is then followed by the recognition of the formed SO_4^{2-} anion by such protonated species, as it is illustrated in Figure 9.

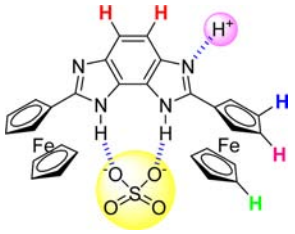

Figure 9. Proposed binding mode for the HSO_4^- anion.

For compound **5**, the detailed evolution of every proton shift, upon addition of the appropriate anion and cation is shown in Figures 10a and 10c, respectively, and in Supporting

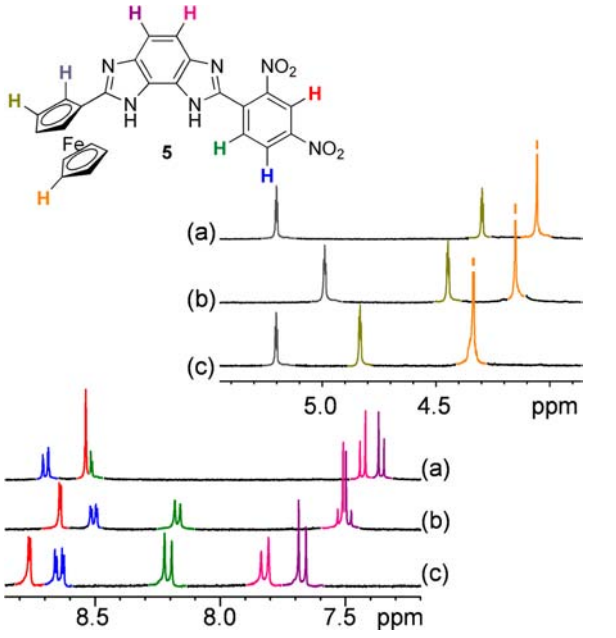

Figure 10. Evolution of the ^{1}H NMR spectrum of the free receptor **5** (b), upon addition of 1 equiv of $[(n\text{-}Bu)_4N]AcO$ (a) and 1 equiv of $Pb(ClO_4)_2$ (c).

Information, Figures S67–S70 as well as in Supporting Information, Table S4. In general, (Figure 10c) protons H4 and H5, appearing at a very close chemical shift in the free receptor (Figure 10b), are split into two clear doublets, shifted to higher field, in the presence of increasing amounts of the anions (AcO^-, $H_2PO_4^-$, HSO_4^-, and SO_4^{2-}). On the other hand, the effect of the anion complexation in the ferrocene protons is dependent on the type of the studied proton. Thus, a shielding effect is observed for both the Hβ, within the

dx.doi.org/10.1021/ic400365c | Inorg. Chem. 2013, 52, 7487–7496

monosubstituted Cp unit, and those within the unsubstituted Cp moiety, while a very pronounced deshielding is observed for the Hα protons. Anion complexation is also accompanied by a significant downfield shift of the ^{1}H NMR signals for the H5′ and H6′ protons of the dinitrophenyl fragment, while the signal for H3′ proton underwent a slight upfield shift.

Regarding the ^{1}H NMR cation titration processes it is worth mentioning the downfield shift detected for all the ferrocenyl, aromatic and heteroaromatic protons present in the free ligand as a result of the cation complexation (Figure 10c and Supporting Information, Figure S70). Interestingly, the protonation effect observed upon addition of HSO_4^- anion to the free ligand **4**, under the ^{1}H NMR titration conditions, is not observed in receptor **5**. This fact is consistent with the lower basicity of the nitrogen atom belonging to the imidazole ring, bearing the electron withdrawing dinitrophenyl substituent.

Because of the limited solubility of **6**, the ^{1}H NMR titration experiments were carried out in THF-d_8 where **6** presents a higher solubility. In particular, a THF-d_8 solution of **6** was titrated with $H_2PO_4^-$, which was added up to 1.2 equiv (see Supporting Information, Figure S71). An analysis of such spectra revealed the following most significant changes: (i) the splitting of the broad signal at δ = 7.43 ppm, corresponding to the protons H4 and H5 protons of the heterocyclic ring, into two doublets [δ = 7.43 ($\Delta\delta$ = 0 ppm) and δ = 7.54 ppm ($\Delta\delta$ = +0.11 ppm)]; (ii) a different behavior of the protons belonging to the ferrocene moiety: while the protons within the unsubstituted Cp ring are unaffected, the Hα are downfield shifted ($\Delta\delta$ = +0.30 ppm) and the Hβ are slightly highfield shifted ($\Delta\delta$ = −0.14 ppm).

CONCLUSIONS

The synthesis of the high flat rigid 2,7-disubstituted benzobisimidazoles **4**–**6** with a large π system, starting from the available 4,5-diamino[2,1,3]benzothiazole as "masked" 1,2,3,4-tetraaminobenzene, is reported. Our synthetic methodology allows the preparation of derivatives bearing different substituents at 2 and 7 positions using the appropriate aldehyde. That means that the heteroaromatic core (ditopic binding site) can be decorated with substituents displaying either redox, chromogenic, or fluorescent properties, which made these new type of receptors potential candidates as multichannel probes for ions. In this sense, the electrochemical, optical, spectroscopic, and sensing properties toward anions and cations have been studied. The bisferrocene-benzobisimidazole triad **4** acts as a dual highly selective redox and fluorescent molecular sensor for HSO_4^- anions and Hg^{2+} cations. The recognition event of the HSO_4^- anion, which probably involves proton transfer followed by hydrogen bond formation and subsequent anion coordination, has been studied by electrochemical, optical techniques, and ^{1}H NMR spectroscopy. Receptor **5** behaves as a redox and chromogenic chemosensor molecule for AcO^-, $H_2PO_4^-$, and SO_4^{2-} anions. The change in the absorption spectra is accompanied by a color change from yellow to orange, which allows their potential "naked eye" detection, whereas Zn^{2+}, Hg^{2+}, and Pb^{2+} cations induced a color change to colorless. Electrochemical data support that the behavior of the HSO_4^- anion is identical to that observed toward receptor **4**. Receptor **6** behaves as redox and chromogenic chemosensor molecule for $H_2PO_4^-$ and AcO^- anions and Zn^{2+}, Cd^{2+}, and Pb^{2+} cations. The perturbations in the absorption spectra after anion addition induced a color change from colorless to yellow. A strong increase of the monomer emission band is observed only in the presence of $H_2PO_4^-$ anions, whereas the fluorescent response toward the metal cations Zn^{2+}, Cd^{2+}, and Pb^{2+} was silent. However, in the presence of the Cu^{2+} and Hg^{2+} metal cations a remarkable increase of the monomeric emission band was observed. In other words, receptor **6** behaves as a fluorescent chemodosimeter of these metal cations.

ASSOCIATED CONTENT

Supporting Information

General experimental comments, NMR spectra, electrochemical, UV–vis, fluorescence, and ^{1}H NMR titration data. This material is available free of charge via the Internet at http://pubs.acs.org.

AUTHOR INFORMATION

Corresponding Author

*E-mail: pmolina@um.es (P.M.), atarraga@um.es (A.T.).

Notes

The authors declare no competing financial interest.

ACKNOWLEDGMENTS

We gratefully acknowledge the financial support from MICINN-Spain, Project CTQ2011/27175, FEDER and Fundación Séneca (Agencia de Ciencia y Tecnología de la Región de Murcia) project 04509/GERM/06 (Programa de Ayudas a Grupos de Excelencia de la Región de Murcia, Plan Regional de Ciencia y Tecnología 2007/2010). One of us M.A. also thanks to the MICINN for a FPI fellowship.

REFERENCES

(1) (a) Kirkovits, G. J.; Shriver, J. A.; Gale, P. A.; Sessler, J. L. *J. Inclusion Phenom. Macrocyclic Chem.* **2001**, *41*, 69–75. (b) Smith, B. D. In *Macrocyclic Chemistry: Current Trends and Future Perspectives*; Gloe, K., Ed.; Springer: Dordrecht, The Netherlands, 2005; (c) Zhu, K.; Zhang, M.; Wang, Z.; Li, N.; Li, S.; Huang, F. *New. J. Chem.* **2008**, *32*, 1827–1830. (d) Zhu, K.; Li, S.; Wang, F.; Huang, F. *J. Org. Chem.* **2009**, *74*, 1322–1328. (e) Zhu, K.; Wu, L.; Yan, X.; Zheng, B.; Zhang, M.; Huang, F. *Chem.—Eur. J.* **2010**, *16*, 6088–6098. (f) Kim, S. K.; Sessler, J. L. *Chem. Soc. Rev.* **2010**, *39*, 3784–3809. (g) McConnell, A. J.; Beer, P. D. *Angew. Chem., Int. Ed.* **2012**, *51*, 5052–506. (h) Hiyaji, H.; Collison, S. R.; Prokes, I.; Tucker, J. H. R. *Chem. Commun.* **2003**, 64–65.

(2) Winnick, F. M. *Chem. Rev.* **1993**, *93*, 587–614.

(3) (a) Nishizawa, S.; Kato, A.; Teramae, N. *J. Am. Chem. Soc.* **1999**, *121*, 9463–9464. (b) Martínez, R.; Espinosa, A.; Tárraga, A.; Molina, P. *Org. Lett.* **2005**, *7*, 5869–5872.

(4) Molina, P.; Tárraga, A.; Otón, F. *Org. Biomol. Chem.* **2012**, *10*, 1711–1724.

(5) (a) Khramov, D. M.; Boydston, A. J.; Bielawski, C. W. *Org. Lett.* **2006**, *8*, 1831–1843. (b) Tennyson, A. G.; Kamplain, J. W.; Bielawski, C. W. *Chem. Commun.* **2009**, 2124–2126. (c) Boydston, A. J.; Williams, K. A.; Bielawski, C. W. *J. Am. Chem. Soc.* **2005**, *127*, 12496–12497. (d) Boydston, A. J.; Pecinovsky, C. S.; Chao, S. T.; Bielawski, C. W. *J. Am. Chem. Soc.* **2007**, *129*, 14550–14551. (e) Boydston, A. J.; Vu, P. D.; Dykhno, O. L.; Chang, V.; Wyatt, A. R., II; Stocketty, A. S.; Ritschdorff, E. T.; Shear, J. B.; Bielawsky, C. W. *J. Am. Chem. Soc.* **2008**, *130*, 3143–3156. (f) Cipollini, M.; Heynderickx, A.; Laurel, F.; Terrier, A.; Jacquemin, D.; Siri, O.; Ortica, F.; Favaro, G. *J. Phys. Chem. C* **2011**, *115*, 23096–23106.

(6) Khramov, D. M.; Boydston, A. J.; Bielawski, C. W. *Angew. Chem., Int. Ed.* **2006**, *45*, 6186–6189.

(7) Park, J. S.; Karnas, E.; Ohkubo, K.; Chen, P.; Kadish, K. M.; Fukuzumi, S.; Bielawski, C. W.; Hudnall, T. W.; Lynch, V. M.; Sessler, J. L. *Science* **2010**, *329*, 1324–1327.

(8) Guo, Z.; Song, N. R.; Moon, J. H.; Kim, M.; Jun, E. J.; Choi, J.; Lee, J. Y.; Bielawski, C. W.; Sessler, J. L.; Juyoung Yoon, J. *J. Am. Chem. Soc.* **2012**, *134*, 17846−17849.
(9) Zapata, F.; Caballero, A.; Tárraga, A.; Molina, P. *J. Org. Chem.* **2010**, *75*, 162−169.
(10) Zapata, F.; Caballero, A.; Espinosa, A.; Tárraga, A.; Molina, P. *Dalton Trans.* **2010**, *39*, 5429−5431.
(11) (a) Mataka, S.; Eguchi, H.; Takahashi, K.; Hatta, K.; Tashiro, M. *Bull. Chem. Soc. Jpn.* **1989**, *62*, 3127−3131. (b) Mataka, S.; Shimojyo, Y.; Hashimoto, I.; Masashi, T. *Liebigs Ann.* **1955**, 1823−1825.
(12) Preliminary communication of this work: Alfonso, M.; Tárraga, A.; Molina, P. *Org. Lett.* **2011**, *13*, 6432−6435.
(13) For reviews see: (a) Molina, P.; Tárraga, A.; Caballero, A. *Eur. J. Inorg. Chem.* **2008**, 3401−3417. (b) Molina, P.; Tárraga, A.; Alfonso, M. *Eur. J. Org. Chem.* **2011**, 4505−4518. (c) Beer, P. D. *Chem. Soc. Rev.* **1989**, *18*, 409−450. (d) Beer, P. D.; Gale, P. A.; Chen. *Coord. Chem. Rev.* **1999**, *185*−*186*, 3−36. (e) Beer, P. D.; Cadman, J. *Coord. Chem. Rev.* **2000**, *205*, 131−155. (f) Beer, P. D.; Hayes, R. J. *Coord. Chem. Rev.* **2003**, *240*, 167−189. (g) Beer, P. D.; Bayly, S. R. *Top. Curr. Chem.* **2005**, *255*, 125−162.
(14) For selective sensing of Pb^{2+} see: (a) Zapata, F.; Caballero, A.; Espinosa, A.; Tárraga, A.; Molina, P. *Org. Lett.* **2008**, *10*, 41−44. For Zn^{2+} see: (b) Zapata, F.; Caballero, A.; Espinosa, A.; Tárraga, A.; Molina, P. *Org. Lett.* **2007**, *9*, 2385−2388. For Hg^{2+} see: (c) Alfonso, M.; Tarraga, A.; Molina, P. *Dalton Trans.* **2010**, *39*, 8637−8645. For AcO^- see: (d) Sola, A.; Tárraga, A.; Molina, P. *Dalton Trans.* **2012**, *41*, 8401−8509. For $H_2PO_4^-$, and $HP_2O_7^{3-}$ see: (e) Zapata, F.; Caballero, A.; Tárraga, A.; Molina, P. *J. Org. Chem.* **2010**, *75*, 162−169.
(15) Plenio, H.; Yang, J.; Diodone, R.; Huinze. *J. Inorg. Chem.* **1994**, *33*, 4098−4104.
(16) Eseola, A. O.; Adepitan, O.; Görls, H.; Plass, W. *New J. Chem.* **2012**, *36*, 891−902.
(17) Alfonso, M.; Tárraga, A.; Molina, P. *J. Org. Chem.* **2011**, *76*, 939−947.
(18) Cillo, C. M.; Lash, T. D. *J. Heterocycl. Chem.* **2004**, *41*, 955−962.
(19) Alfonso, M.; Sola, A.; Caballero, A.; Tárraga, A.; Molina, P. *Dalton Trans.* **2009**, 9635−9658.
(20) OSWV technique has been employed to obtain well-resolved potential information, while the individual redox processes are poorly resolved in the CV experiments in which individual $E_{1/2}$ potentials cannot be easily or accurately extracted from these data: (a) Serr, B. R.; Andersen, K. A.; Elliot, C. M.; Anderson, O. P. *Inorg. Chem.* **1988**, *27*, 4499−4504. (b) Richardson, D. E.; Taube, H. *Inorg. Chem.* **1981**, *20*, 1278−1285.
(21) Amendola, V.; Esteban-Gómez, D.; Fabrizzi, L.; Licchelli, M. *Acc. Chem. Res.* **2006**, *39*, 343−353.
(22) (a) Descalzo, A. B.; Rurack, K.; Weisshof, H.; Martínez-Máñez, R. M.; Marcos, M. D.; Amorós, P.; Hoffmann, K.; Soto, J. *J. Am. Chem. Soc.* **2005**, *127*, 184−200. (b) Vázquez, M.; Fabbrizzi, L.; Taglietti, A.; Pedrido, R. M.; González-Noya, A. M.; Bermejo, M. R. *Angew. Chem., Int. Ed.* **2004**, *43*, 1962−1965. (c) Boiocchi, M.; Dal Boca, L.; Esteban-Gómez, D.; Fabbrizzi, L.; Licchelli, M.; Monzani, E. *J. Am. Chem. Soc.* **2004**, *126*, 16507−16514. (d) Esteban-Gómez, D.; Fabbrizzi, L.; Licchelli, M.; Monzani, E. *Org. Biomol. Chem.* **2005**, *3*, 1495−1500. (e) Evans, L. S.; Gale, P. A.; Light, M. E.; Quesada, R. *Chem. Commun.* **2006**, 965−967. (f) Camiolo, S.; Gale, P. A.; Hursthouse, M. B.; Light, M. E. *Org. Biomol. Chem.* **2003**, *1*, 741−744. (g) Camiolo, S.; Gale, P. A.; Hursthouse, M. B.; Light, M. E.; Shi, A. J. *Chem. Commun.* **2002**, 758−759. (h) Gale, P. A.; Navakhun, K.; Camiolo, S.; Light, M. E.; Hursthouse, M. B. *J. Am. Chem. Soc.* **2002**, *124*, 11228−11229. (i) He, X.; Hu, S.; Liu, K.; Guo, Y.; Xu, J.; Shao, S. *Org. Lett.* **2006**, *8*, 333−336. (j) Viruthachalam, T.; Ramamurthy, P.; Thirumalai, D.; Ramakrishman, V. *Org. Lett.* **2005**, *7*, 657−660. (k) Caltaginore, C.; Bate, G. W.; Gale, P. A.; Light, M. E. *Chem. Commun.* **2008**, 61−63.
(23) (Specfit/32 Global Analysis System, 1999−2004 Spectrum Software Associates (SpecSoft@compuserve.com). The Specfit program was adquired from Biologic, SA (www.bio-logic.info) in January 2005. The equation to be adjusted by nonlinear regression, using the above-mentioned software was the following: $\Delta A/b = \{K_{11}\Delta\varepsilon_{HG}[H]_{tot}[G]\}/\{1 + K_{11}[G]\}$, where H = host, G = guest, HG = complex, ΔA = variation in the absorption, b = cell width, K_{11} = association constant for a 1:1 model, and $\Delta\varepsilon_{HG}$ = variation of molar absorptivity.
(24) (a) Zapata, F.; Caballero, A.; Espinosa, A.; Tárraga, A.; Molina, P. *J. Org. Chem.* **2008**, *73*, 4034−4044. (b) Alfonso, M.; Tárraga, A.; Molina, P. *J. Org. Chem.* **2011**, *63*, 939−947.
(25) Miller, S. R.; Gustwski, D. A.; Chen, Z. H.; Gokel, G. H.; Echegoyen, L.; Kaifer, A. E. *Anal. Chem.* **1988**, *60*, 2021−2024.
(26) (a) Beer, P. D.; Graydon, A. R.; Johnson, A. O. M.; Smith, D. K. *Inorg. Chem.* **1997**, *36*, 2112−2118. (b) Otón, F.; Tárraga, A.; Espinosa, A.; Velasco, M. D.; Molina, P. *J. Org. Chem.* **2006**, *71*, 4590−4598. (c) Otón, F.; Tárraga, A.; Molina. *Org. Lett.* **2006**, *8*, 2107−211. (d) Otón, F.; Espinosa, A.; Tárraga, A.; Ramírez de Arellano, C.; Molina, P. *Chem.—Eur. J.* **2007**, *13*, 5742−5752.
(27) Dawson, W. R.; Windsor, M. W. *J. Phys. Chem.* **1968**, *72*, 3251−3260.
(28) CHEF is defined as I_{max}/I_0, where I_{max} corresponds to the maximum emission intensity of the receptor-metal species formed, while I_0 is the maximum emission intensity of the free receptor.
(29) Shortreed, M.; Kopelman, R.; Kuhn, M.; Hoyland, B. *Anal. Chem.* **1996**, *68*, 1414−1418.
(30) (a) Evans, A. J.; Watkins, S. E.; Craig, C.; Colbran, S. B. *J. Chem. Soc., Dalton Trans.* **2002**, 983−994. (b) Potts, K. T.; Keshavarz-K, M.; Tham, F. S.; Abruña, H. D.; Arana, C. R. *Inorg. Chem.* **1993**, *32*, 4422−4435. (c) Cui, X.; Carapuca, H. M.; Delgado, R.; Drew, M. G. B.; Felix, V. *Dalton Trans.* **2004**, 1743−1751. (d) Otón, F.; Tárraga, A.; Espinosa, A.; Velasco, M. D.; Molina, P. *Dalton Trans.* **2006**, 3685−3692. (e) Sato, M.; Katada, M.; Nakashima, S.; Sano, H. *J. Chem. Soc., Dalton Trans.* **1990**, 1979−1984. (f) Plenio, H.; Aberle, C.; Shihadeh, Y. A.; Lloris, J. M.; Martínez-Máñez, R.; Pardo, T.; Soto, J. *Chem.—Eur. J.* **2001**, *7*, 2848−2861.
(31) (a) Martínez, R.; Ratera, I.; Tárraga, A.; Molina, P.; Veciana, J. *Chem. Commun.* **2006**, 3809−3811. (b) Zapata, F.; Caballero, A.; Espinosa, A.; Tárraga, A.; Molina, P. *Dalton Trans.* **2009**, 3900−3900. (c) Romero, T.; Caballero, A.; Tárraga, A.; Molina, P. *Org. Lett.* **2009**, *11*, 3466−3469.